Quaternary Research 70 (2008) 451–464

Contents lists available at ScienceDirect

Quaternary Research

journal homepage: www.elsevier.com/locate/yqres

Orbital- and sub-orbital-scale climate impacts on vegetation of the western Mediterranean basin over the last 48,000 yr

William J. Fletcher *, Maria Fernanda Sánchez Goñi

Ecole Pratique des Hautes Etudes, UMR 5805 CNRS EPOC, Université Bordeaux 1, Avenue des Facultés, 33405 Talence Cedex, France

ARTICLE INFO

Article history:
Received 13 December 2007
Available online 7 September 2008

Keywords:
Marine palynology
Land–sea correlation
Iberian margin
Mediterranean region
Dansgaard-Oeschger variability
Heinrich events
LGM
Holocene
Precession

ABSTRACT

High-resolution pollen analysis of Alborán Sea core MD95-2043 provides a 48-ka continuous vegetation record that can be directly correlated with sea surface and deep-water changes. The reliability of this record is supported by comparison with that of Padul (Sierra Nevada, Spain). Marine Isotope Stage (MIS) 3 was characterised by fluctuations in *Quercus* forest cover in response to Dansgaard-Oeschger climate variability. MIS 2 was characterised by the dominance of semi-desert vegetation. Despite overall dry and cold conditions during MIS 2, Heinrich events (HEs) 2 and 1 were distinguished from the last glacial maximum by more intensely arid conditions. Taxon-specific vegetation responses to a tripartite climatic structure within the HEs are observed. In MIS 1, the Bölling-Allerød was marked by rapid afforestation, while a re-expansion of semi-desert environments occurred during the Younger Dryas. The maximum development of mixed *Quercus* forest occurred between 11.7 and 5.4 cal ka BP, with forest decline since 5.4 cal ka BP. On orbital timescales, a long-term expansion of semi-desert vegetation from MIS 3 into MIS 2 reflects global ice-volume trends, while Holocene arboreal decline reflects summer insolation decrease. The influence of precession on the amplitude of forest development and vegetation composition is also detected.

Introduction

High-resolution multi-proxy studies of marine sediment sequences from the Alborán Sea reveal the sensitivity of marine environments and atmospheric conditions in the western Mediterranean to sub-orbital North Atlantic climate variability associated with abrupt atmospheric changes over Greenland (Dansgaard-Oeschger (D-O) events) and episodes of massive iceberg discharge into the North Atlantic (Heinrich Events, HEs) (Cacho et al., 1999, 2000, 2006; Moreno et al., 2002; Pérez-Folgado et al., 2003; Colmenero-Hidalgo et al., 2004). Previous palynological studies of Alborán Sea sediments in marine cores MD95-2043 and ODP site 976 have shown the sensitive response of the Mediterranean vegetation to rapid climate variability during the last glacial period, with rapid forest development during interstadials and forest contractions accompanied by the expansion of semi-desert vegetation during D-O stadials and HEs (Combourieu Nebout et al., 2002; Sánchez Goñi et al., 2002). The Alborán records document the most strongly arid and cold atmospheric conditions during the HEs, with forest declines of greater amplitude during the HEs than most D-O stadials. Similarly, model–data comparisons also indicate that HE1 was characterised by more arid conditions in the Alborán Sea borderlands than the last glacial maximum (LGM) (Kageyama et al., 2005).

While recurrent patterns of vegetation response to D-O and HE events have been demonstrated in the Alborán records, key questions remain about the nature of vegetation response in this region to climate change at different timescales. First, as orbital-scale vegetation–climate relationships have been little explored in the Alborán data, it remains important to identify long-term controls on vegetation development and to understand whether orbital-scale influences can be detected during periods distinguished primarily by high-amplitude millennial-scale variability. Second, at the sub-orbital scale, the understanding of vegetation response to abrupt climate events may also be improved.

Since the publication of the first pollen records from the Alborán Sea, the complexity of HE impacts on the western Mediterranean region has been revealed by marine proxy records for deep-water formation, with the transmission of climate changes from the North Atlantic region via both atmospheric and oceanic processes. Benthic $\delta^{13}C$ records in particular reveal the complex structure of the HEs, with a general pattern of heavy values during early and late phases of the HEs related to wind-driven enhancement of the Mediterranean thermohaline circulation, and light values during the middle phases reflecting freshening of the surface water and reduced circulation strength due to the entrance of low-salinity sub-polar waters into the Mediterranean (Sierro et al., 2005; Cacho et al., 2006; Frigola et al., 2008). So far, it has not been ascertained whether vegetation changes in the Alborán region are more closely related to the atmospheric or oceanic transmission of HE impacts. Moreover, recent research on the Atlantic margin has shown complex patterns of vegetation response within HEs (Naughton et al.,

* Corresponding author. Fax: +33 5 56 84 08 48.
E-mail address: w.fletcher@epoc.u-bordeaux1.fr (W.J. Fletcher).

0033-5894/$ – see front matter © 2008 University of Washington. All rights reserved.
doi:10.1016/j.yqres.2008.07.002

2007a), but no evidence from the Mediterranean region has been shown for internal patterns within the HEs.

In order to answer these questions, we present here a high-resolution pollen record for Alborán marine core MD95-2043, extending the previous MIS 3 record (Sánchez Goñi et al., 2002) to include the two most recent HEs, the LGM, the deglaciation period and the Holocene. Continuous, high sedimentation rates and a robust radiometric and ice-core correlated chronology permit the investigation of both millennial-scale vegetation dynamics and orbital-scale trends in regional vegetation history. This type of analysis has not previously been possible in a region with few terrestrial records extending beyond the Holocene.

Environmental setting

The Alborán Sea is the western-most basin of the Mediterranean Sea, located between SE Iberia and N Africa (Fig. 1). Marine circulation in the Alborán Sea is governed by the Mediterranean thermohaline circulation system, which results from a negative hydrological balance over the entire basin and the generation of dense water masses (Bethoux, 1979). North Atlantic Surface Water (NASW) enters the Alborán Sea, forming a low-salinity surface current (Modified Atlantic Water, MAW) that defines two anticyclonic gyres before flowing eastward into the Mediterranean along the Algerian coast (Millot, 1999). At deeper levels of the water column, dense saline currents of the Levantine Intermediate Water (LIW) and Western Mediterranean Deep Water (WMDW) flow westwards to produce the Mediterranean Outflow Water as they enter the Atlantic. LIW forms in the eastern Mediterranean due to evaporation and sinking of MAW, while WMDW forms in the Gulf of Lions, driven by winter cooling of the surface waters by westerly winds in this region (Millot, 1999).

The lands bordering the Alborán Sea are dominated by an arc of mountain ranges composed of the Baetic Sierras (Spain) and the Rif (Morocco), with peaks over 2400 m in the Rif and 3400 m in the highest range of the Baetic Sierras, the Sierra Nevada. The climate of the Alborán borderlands is Mediterranean, with hot, dry summers governed by the strength of the Azores anticyclone, and mild, humid winters influenced by mid-latitude atmospheric circulation patterns and the position of Atlantic storm tracks. Predominant wind directions are westerly and northwesterly during winter, with southerly and southwesterly winds occurring during summer associated with weakening of the westerlies. Altitudinal contrasts yield a wide range of regional thermal conditions (thermomediterranean to cryomediterranean), with mean annual temperatures ranging from more than 20°C at sea-level to less than 10°C for the highest areas (Arévalo Barroso, 1992). Regional precipitation patterns are strongly influenced by the westerly origin of Atlantic moisture and the orographic complexity of the neighbouring landmasses, with annual precipitation values ranging from >1400 mm/yr in the western highlands of the Rif and Baetic Sierras to <400 mm/yr in the eastern lowlands of Almeria and the Moulouya basin (Morocco).

Forest vegetation in the Alborán borderlands reflects thermal and pluvial gradients related to increasing altitude and maritime influence (Peinado Lorca and Rivas-Martinez, 1987; Benabid, 2000; Quezel, 2002). Sclerophyllous shrublands and evergreen oak formations predominate at low altitudes (up to ~1200 m), while mixed evergreen/deciduous and deciduous oak forest formations occur at mid-altitudes (~1200–1800 m) and with increased moisture availability. Coniferous vegetation is well developed at higher altitudes, including pines (*Pinus* spp.), junipers (*Juniperus thurifera* and *J. communis* ssp. nana), and, in North Africa, cedar (*Cedrus atlantica*). The highest altitudes (above ~2200 m) display juniper formations, shrublands of cushion-form xerophytes, and pasturelands. The driest areas (<250 mm/yr) in both the lowland plains or high altitude plateaus display the development of steppe, either grass steppe dominated by *Stipa tenacissima*, or chamaephytic steppe dominated by *Artemisia herba-alba*. In this paper we use the term semi-desert to refer to these Mediterranean steppe environments, and include the pollen types *Artemisia*, Chenopodiaceae and *Ephedra distachya* type.

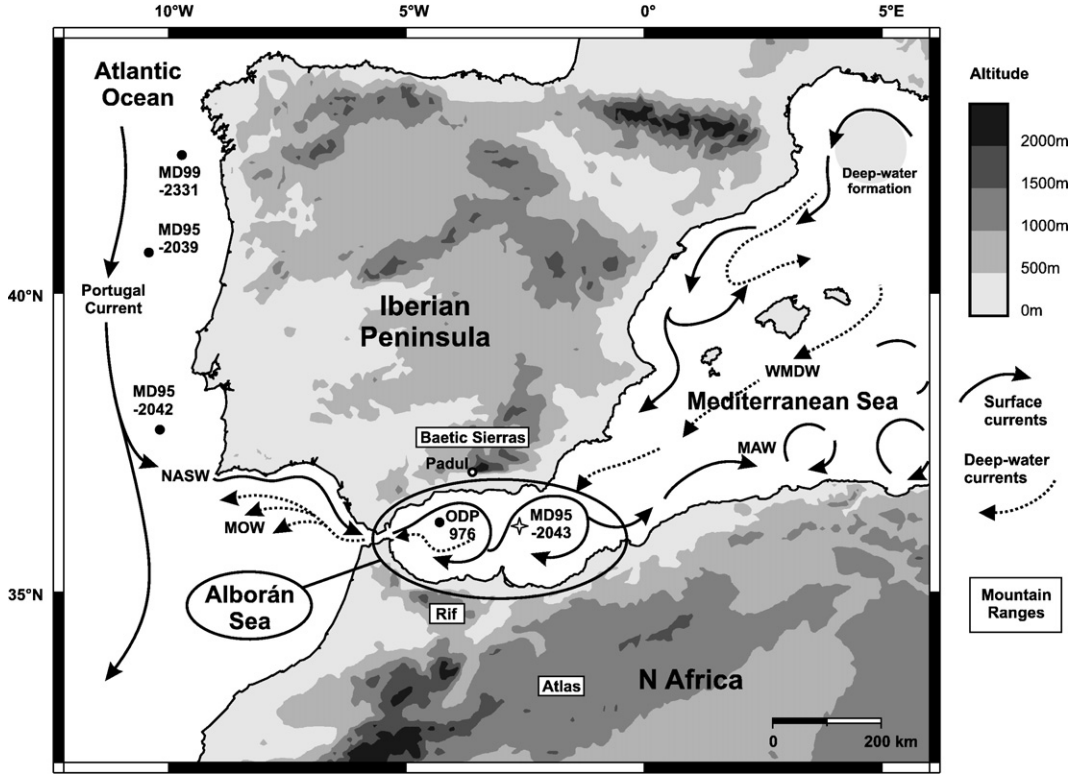

Figure 1. Location of the Alborán Sea and marine core MD95-2043, and key sites mentioned in the text, namely marine cores MD99-2331 (Naughton et al., 2007a), MD95-2039 (Roucoux et al., 2005), MD95-2042 (Sánchez Goñi et al., 2000), ODP site 976 (Combourieu Nebout et al., 2002), and the terrestrial site of Padul (Pons and Reille, 1988). Principal surface and deep-water currents redrawn from Millot (1999).

https://doi.org/10.1016/j.yqres.2008.07.002 Published online by Cambridge University Press

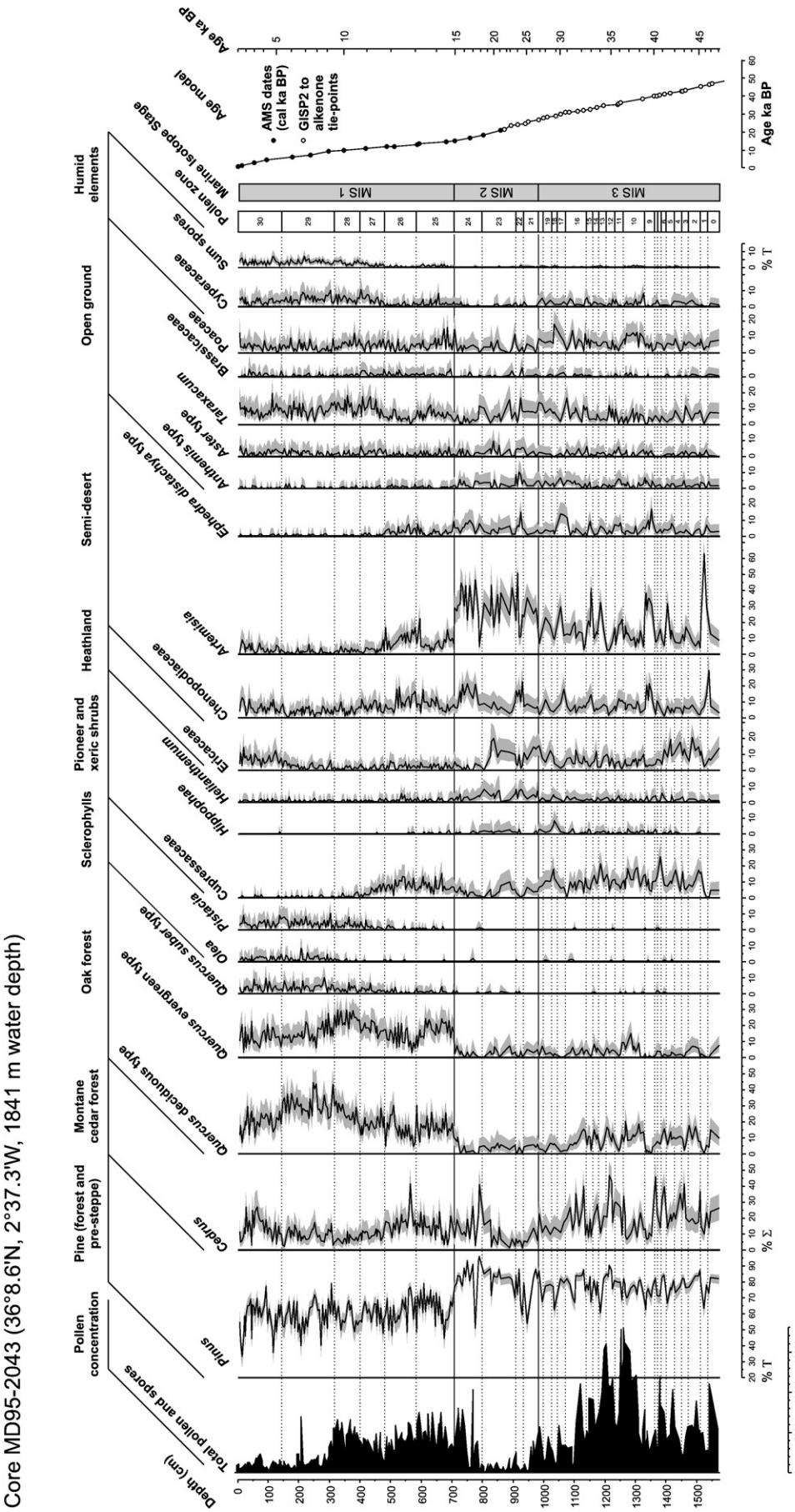

Figure 2. Pollen diagram against depth, showing pollen concentration (total pollen and spores) and pollen percentage values calculated on the basis of the main pollen sum (%Σ), except for *Pinus* and spores which are calculated against the total sum of all pollen and spores (%T). 95% confidence intervals for pollen percentage values (following Maher, 1972) are shown in grey. The age–depth curve shows the placement of control points following the age model of Cacho et al. (1999).

https://doi.org/10.1016/j.yqres.2008.07.002 Published online by Cambridge University Press

Grass steppe is not considered likely to have a clear palynological signal as members of the Poaceae family also occur in a wide range of other habitats.

Materials and methods

The deep-sea core MD95-2043 (36°8.6′N, 2°37.3′W, 1841 m water depth) was recovered in the Alborán Sea using a CALYPSO corer on the R/V *Marion Dufresne* during the 1995 IMAGES-I oceanographic campaign. The present study concerns the top 16 m of the core, which represents a sequence of fine-grained hemipelagic sediments corresponding to the last 48,000 yr. The age model for MD95-2043 is presented in Cacho et al. (1999) and is based on 17 calibrated AMS radiocarbon dates for the upper part (corresponding to the last 21 cal ka BP) and visual correlation between the alkenone sea surface temperature record of this core and the GISP2 $\delta^{18}O$ curve for the lower part. Here, while the placement of age–depth control points remains unchanged from Cacho et al. (1999), the upper part of the age–depth curve as shown in Figure 2 is slightly altered as we have recalibrated the radiocarbon dates against the Marine04 calibration curve (Hughen et al., 2004) implemented in CALIB (Stuiver and Reimer, 1993; version 5.02). Ages based on this age model combining calibrated radiocarbon and ice-core chronological data are reported as ka BP (equivalent to calendar years before AD 1950). Average temporal resolution for the pollen record is ~180 yr.

Sediment subsamples of 1-cm thickness and 2–8 cm^3 volume were prepared for pollen analysis using the standard protocol employed at Université Bordeaux 1 for marine samples, employing coarse-sieving at 150 μm, successive treatments with cold HCl at increasing strength (10%, 25% and 50%), successive treatments with cold HF (HF 25% for 2 1/2 h, HF 70% 1 1/2 days), and micro-sieving (10 μm mesh). Known quantities of *Lycopodium* spores in tablet form were added to permit the calculation of pollen concentrations. Slides were prepared using a mobile mounting medium to permit rotation of the grains and counted using a Zeiss Axio Imager A10 light microscope at 400× magnification with routine use of 1000× magnification for the identification of pollen and spores. Pollen counts aimed to reach at least 20 taxa and a main sum of 100 terrestrial pollen grains excluding *Pinus*, aquatics and spores. For 26 out of 288 samples, concentrated chiefly in the core section corresponding to MIS 2, the main sum could not be reached due to very low pollen concentration; these samples are included in the pollen concentration curve but are excluded from pollen percentage curves and all other analyses.

Pollen percentages for terrestrial taxa are calculated against the main sum of terrestrial grains, while percentages for *Pinus*, aquatics and spores are calculated against the total sum of all pollen and spores. The main sum of 100 terrestrial grains is relatively low in comparison with the standard counts of at least 300 (and frequently much higher) employed in the analysis of terrestrial sites. However, the low concentration of pollen and spores in marine sediments (typically $<10^4$ grains/cm^3, Fig. 2) means that higher counts are not achievable. While the abundance of *Pinus* yields total pollen and spore counts that are fairly large (mean count for this dataset, 504), the exclusion of *Pinus* from the main sum implies that the error associated with the calculated pollen percentage values (being dependent on the size of the pollen sum and the proportion of a given pollen type) may be fairly large. For the MD95-2043 dataset, 95% confidence intervals (following Maher, 1972) for non-zero values range between 3.2 and

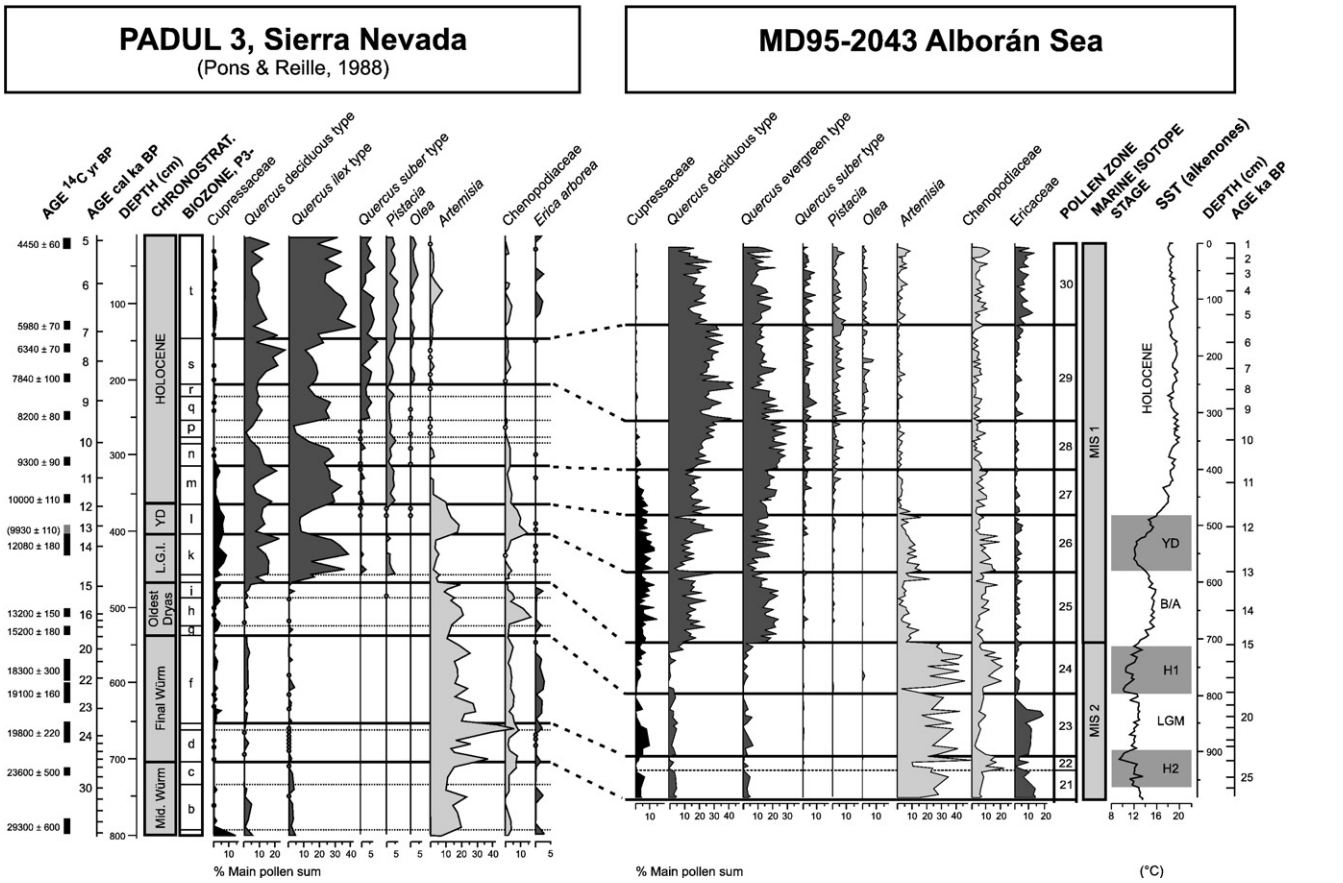

Figure 3. Comparison of pollen records from Padul in the Sierra Nevada (Baetic Sierras), Spain (redrawn from Pons and Reille, 1988) and MD95-2043. A calibrated age scale has been added to the Padul diagram, using a model of linear interpolation and radiocarbon data published in Pons and Reille (1988), excluding one date shown in grey. Alkenone SST data for MD95-2043 from Cacho et al. (1999).

https://doi.org/10.1016/j.yqres.2008.07.002 Published online by Cambridge University Press

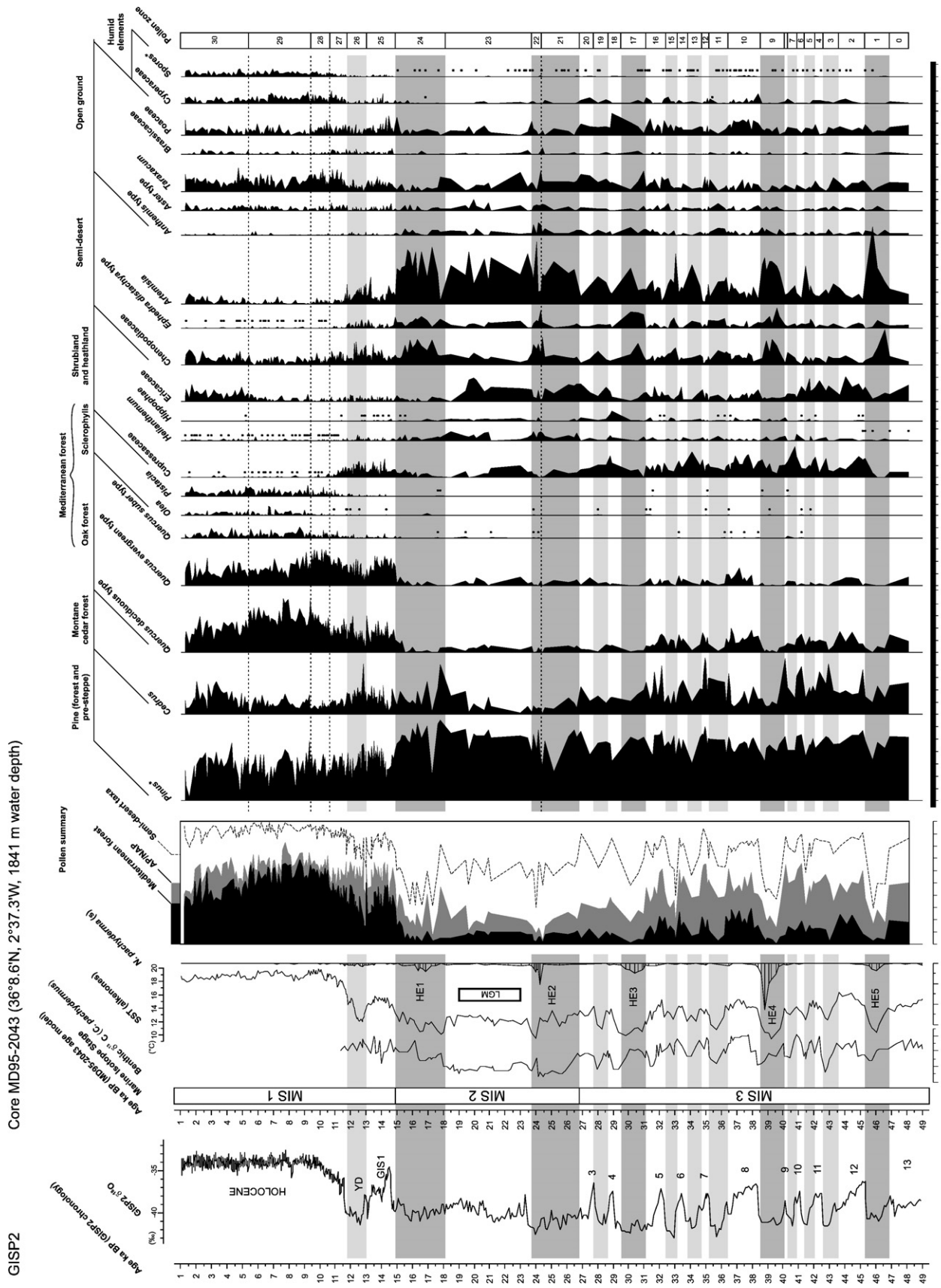

Figure 4. Pollen diagram against age, shown with marine proxy records from the same core and the GISP2 oxygen isotope curve from Grootes et al. (1993). Benthic $\delta^{13}C$ values from Cacho et al. (2002, 2006); alkenone SST reconstruction and *N. pachyderma* (s) abundances from Cacho et al. (1999). Pollen summary curves shown for Mediterranean forest (including all pollen types typical of the thermomediterranean to supramediterranean altitudinal forests, namely *Acer*, *Alnus*, *Betula*, *Corylus*, *Fraxinus excelsior* type, *Populus*, *Taxus*, *Ulmus*, *Quercus* deciduous type, *Quercus* evergreen type, *Quercus suber* type, *Cistus*, *Coriaria myrtifolia*, *Olea*, *Phillyrea*, and *Pistacia*), for arboreal pollen (including all woody taxa except *Pinus*), and for semi-desert vegetation (including *Artemisia*, Chenopodiaceae and *Ephedra distachya* type). Shaded pollen zones correspond to Greenland stadials (light grey) and Heinrich events (dark grey).

https://doi.org/10.1016/j.yqres.2008.07.002 Published online by Cambridge University Press

25.1% (mean value 7.9%). These broad confidence intervals suggest that the interpretation of small shifts in percentage values or the behaviour of taxa represented at very low values must be extremely cautious. Nevertheless, in plotting the pollen curves with the 95% confidence intervals, it is apparent that both abrupt changes and longer-term trends in pollen percentage curves are salient regardless of uncertainties derived from the smaller pollen sum employed in marine palynology (Fig. 2).

A total of 105 pollen and spore taxa were identified in the MD95-2043 samples. Thirty-one pollen zones have been defined by visual inspection of the pollen curves on the basis of coincident changes occurring in multiple pollen taxa (Fig. 2). To aid discussion of the marine proxy and pollen records, we make use of LOWESS, or locally weighted regression scatterplot smoothing (Cleveland, 1979), a non-parametric regression technique implemented in the program Minitab. LOWESS provides a useful graphical summary of patterns of change in stratigraphical data where no single functional relationship (e.g., linear or quadratic) is apparent (Birks, 1998). The degree of smoothing (in this case, α=0.3) was selected judgmentally so as best to display long-term tendencies while minimising "noise" related to millennial-scale variability in the data.

Results and Interpretation

Comparison with Padul and implications for pollen source areas

Before considering vegetation–climate relationships, a comparison is presented with the well-known record from Padul (core P3, Fig. 3), a peat-bog site located at 785 m altitude in the Sierra Nevada range of the Baetic Sierras and approximately 150 km from the MD95-2043 core location. The two records show strong similarities in the curves for major taxa representing Mediterranean forest, shrubland and semi-desert vegetation over the last 25 ka BP. Comparison for the period 25–50 ka BP is not worthwhile as the effective temporal resolution in the upper part of Padul core P2 is extremely low and stadial/interstadial variability is not apparent. Important similarities include parallel increases in Chenopodiaceae pollen and sustained percentages of *Artemisia* during the Oldest Dryas (recently shown to be the terrestrial equivalent to HE 1 (Naughton et al., 2007a)), major expansion of mixed *Quercus* forest at the onset of the Bölling, high values of Cupressaceae during the Bölling/Allerød and Younger Dryas, and modest increases in Ericaceae and *Artemisia* during the late Holocene. Many other shared features in both major and minor taxa may be noted, including the decline of Cupressaceae in the early to mid-Holocene, the rise of *Quercus suber* and *Olea* during the mid-Holocene, and the decline of deciduous *Quercus* in the late Holocene. Interestingly, the marked reduction of *Quercus* pollen values in Padul zones P3o and P3p (reflecting a peak in Poaceae and monolete spores) is not recorded in the MD95-2043 diagram, supporting the original authors' interpretation that this represents a local event only at the Padul site.

Several studies of marine sediment surface samples have shown that terrestrial pollen and spores in marine sediments represent an integrated, regional-scale image of vegetation in the adjacent continental areas (Heusser and Balsam, 1977; Turon, 1984; Mudie et al., 2002; Mudie and McCarthy, 2006; Hooghiemstra et al., 2006; Naughton et al., 2007a). The strong similarities with the Padul record suggest that the MD95-2043 record represents a reliable integrated image of vegetation in the Baetic zone of southern Spain. Why this should be the case may be related to a prevailing dominance of fine sediment supply to the Alborán basin via fluvial sources from the Iberian borderlands (Fabrés et al. 2001), and/or a predominance of northwesterly winds during pollination periods (winter to early summer). Nevertheless, the abundance of *Cedrus* in the MD95-2043 spectra reveals an indisputable North African pollen component, probably resulting from periodic winds of North African origin, though also perhaps from fluvial transport of pollen in northward flowing rivers draining the Moroccan Rif. The abundance of *Cedrus* implies that an unknown proportion of other pollen types may also originate from the southern Alborán borderlands, and that ultimately the MD95-2043 record represents an integrated image of both the Iberian and North African borderlands. In this case, one implication of the strong similarity with the Padul record would be that the Mediterranean zones of Spain, Morocco and W. Algeria share broadly similar vegetation histories— a conclusion that is plausible given the general similarities in modern vegetation composition and zonation in these regions.

Overview of vegetation changes since 48 ka BP

MIS 3 in the MD95-2043 pollen record (48.1 to 26.8 ka BP) is characterised by the dynamic opposition between phases of alternating forest development and semi-desert expansion in phase with warming and cooling of sea surface temperatures, respectively (Fig. 4). As previously discussed (Sánchez Goñi et al. 2002; Combourieu Nebout et al., 2002), the dynamic behaviour of forest vegetation in the Alborán borderlands during this period can be correlated with the record of Dansgaard-Oeschger (D-O) climate variability over Greenland, with expansions of mixed oak forest (deciduous and evergreen *Quercus*) during interstadials, and expansions of semi-desert vegetation (*Artemisia*, Chenopodiaceae and *Ephedra distachya* type) during stadials and HEs (which, in the absence of ice-rafted detritus, are distinguished by the elevated percentages of the cold water foraminifer *N. pachyderma* (s), high-amplitude SST reductions, and heavy isotopic values for $\delta^{13}C$ corresponding to enhanced deep-water circulation (Cacho et al, 1999, 2006)). In general, forest decline and semi-desert expansion was more marked during HEs than during other MIS 3 stadials (Fig. 5). Contrasts between groups of interstadials can be observed, namely that the earlier interstadials in the record (GIS 12–9) are marked by an important development of Ericaceae (heaths), the subsequent interstadials (GIS 8–5) by more frequent occurrences of thermomediterranean taxa, and the later interstadials (GIS 4, 3) by a limited development of *Quercus* forest. These contrasts can be more clearly seen comparing directly GIS 12, 8 and 4–3 (Fig. 6).

For the period 26.8–14.9 ka BP, equivalent to MIS 2, the pollen spectra suggest an open landscape dominated by semi-desert vegetation (*Artemisia*-rich steppe) and cryo-xeric shrub formations with Cupressaceae and *Helianthemum*. Refugial populations of oaks, both deciduous and evergreen, were present in the region, confirming

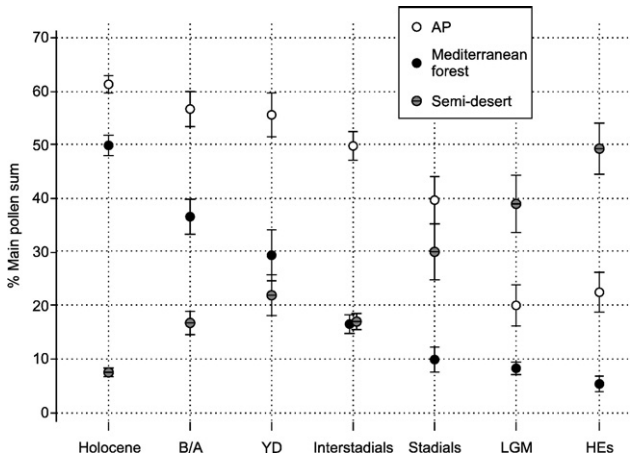

Figure 5. Interval plot of mean values for arboreal pollen, Mediterranean forest and semi-desert taxa, showing 95% confidence intervals for the means. Summary groups as defined in Figure 4. Values are calculated for the following groups: Holocene (pollen zones 27–30), Bölling-Allerød (pollen zone 25), Younger Dryas (pollen zone 26), MIS 3 interstadials (pollen zones 0, 2, 4, 6, 8, 10, 12, 14, 16, 18, 20), MIS 3 stadials (pollen zones 3, 5, 7, 11, 13, 15, 19), the LGM (pollen zone 23), and Heinrich events 1–5 (pollen zones 1, 9, 17, 21–22, 24).

https://doi.org/10.1016/j.yqres.2008.07.002 Published online by Cambridge University Press

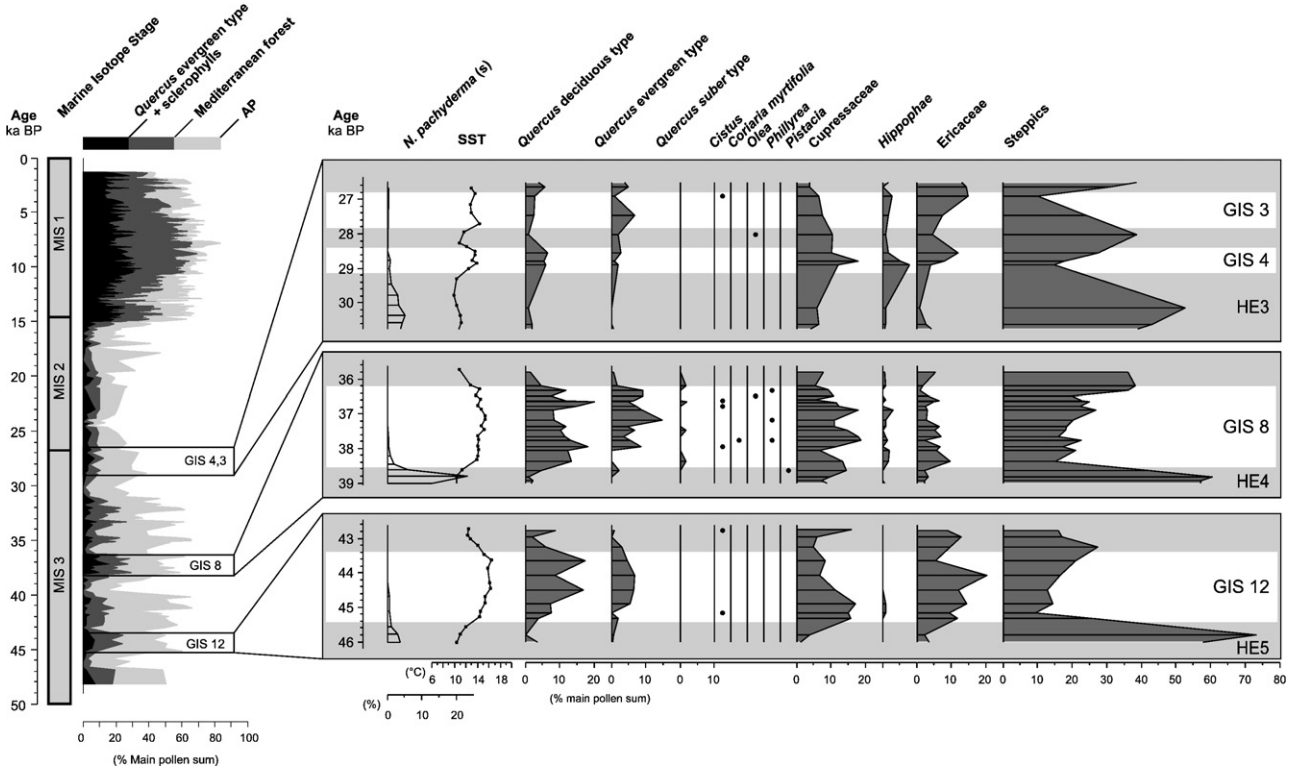

Figure 6. Comparison of pollen spectra corresponding to GIS 12, 8, and 4–3, accompanied by a summary curve showing arboreal and Mediterranean forest groups as defined in Figure 4.

terrestrial fossil evidence, molecular evidence and modelling predictions (Brewer et al., 2002; Olalde et al., 2002; Benito Garzón et al., 2007; López de Heredia et al., 2007). Although sample resolution is lower in this section due to low pollen concentration effects, an important distinction can nevertheless be made between the Heinrich events (HEs 2 and 1) and the last glacial maximum (LGM), taken here as 19–23 cal ka BP following EPILOG and MARGO (Mix et al., 2001; Kucera et al., 2005). The strongest reductions of arboreal pollen and expansions of semi-desert vegetation occur during HEs 2 and 1, while during the LGM slightly more humid conditions permitted the development of shrubby vegetation formations with Cupressaceae, *Helianthemum*, *Hippophäe* and Ericaceae. The maximum expansion of semi-desert taxa in pollen zones 22 and 24 is associated with the main entrance of sub-polar waters into the Alborán Sea as indicated by peak values for *N. pachyderma* (s). However, the onset of the HE 2, as recorded in deep-water circulation changes, occurs during a transitional pollen zones (21) preceding the maximum in semi-desert taxa. The LGM, showing modest values for arboreal pollen and high values for semi-desert taxa, suggests a cooler and drier climate than most MIS 3 stadials, but nevertheless warmer and wetter than that prevailing during HEs (Fig. 5). Semi-desert taxa are better represented during the LGM in the MD95-2043 record than at ODP site 976 (Kageyama et al., 2005), suggesting a west-to-east gradient of increasing aridity across the Alborán basin.

MIS 1 in the pollen record (after 14.9 cal ka BP) is characterised overall by well-developed Mediterranean mixed oak forests and the contraction of formerly widespread areas of *Artemisia*-rich steppe. Rapid afforestation by evergreen and deciduous *Quercus* is recorded at the onset of the Bölling in phase with SST warming, and confirms the nature and timing of patterns observed in regional terrestrial sequences in the Baetic Sierras (Pons and Reille, 1988; Fernández et al., 2007) and in SW Iberia (Fletcher et al., 2007). A re-expansion of semi-desert taxa and the contraction of *Quercus* forest is recorded during the Younger Dryas, indicating atmospheric cooling and drying in phase with SST cooling. However, while YD SSTs fall to within the range of LGM and D-O stadial temperatures (11–13°C, Cacho et al., 1999), the decline of arboreal populations was much less marked than that occurring during the LGM or D-O stadials (Fig. 5). A peak in *Cedrus* pollen during the YD may indicate a positive response of montane forest vegetation in North Africa to regional cooling, as observed in the Algerian Atlas (Salamani, 1993).

The early to mid-Holocene (11.7–5.4 cal ka BP) was characterised by maximum development of *Quercus* forest, with changes in forest composition reflecting a shift in climatic regime at around 9.4 ka BP. The early Holocene record (11.7–9.4 cal ka BP) is marked by high values of evergreen *Quercus*, accompanied by Cupressaceae and *Artemisia*, while the period from 9.4 to 5.4 cal ka BP reveals a stronger representation of deciduous oaks, accompanied by cold-sensitive taxa: *Quercus suber* type, *Olea* and *Pistacia*. The pattern is consistent with changes in evergreen/deciduous oak proportions over the early to mid-Holocene observed in lowlands of SW Iberia (Fletcher et al., 2007) and in the Middle Atlas of Morocco (Lamb and van der Kaars, 1995). The vegetation changes suggest a climatic transition from continental/dry to oceanic/moist conditions related to a gradual reduction in seasonal contrast (cooler summers and warmer winters). The latter, more oceanic phase includes the mid-Holocene mesophytic forest maximum identified in SE Iberian continental records (Carrión et al., 2007, 2004, 2003, 2001; Carrión 2002).

The pollen record for the late Holocene (5.4–1.3 cal ka BP) indicates a decline of deciduous *Quercus* and an increase in Ericaceae, reflecting a pattern of upland forest decline as recorded in terrestrial sequences of the Baetic Sierras (Carrión, 2002; Carrión et al., 2007, 2004, 2003; Fernández et al., 2007). An expansion of semi-desert is also recorded, corroborating the steppe expansion observed in the semi-arid Almeria lowlands (Pantaléon Cano et al., 2003). The record also suggests late Holocene *Cedrus* population expansions at the expense of deciduous oak, consistent with several terrestrial records from the Moroccan Rif and Middle Atlas (Reille, 1977; Lamb and van der Kaars, 1995). These combined changes suggest an overall cooling trend since 5.4 cal ka BP, accompanied by drying at lower altitudes but with sufficient

https://doi.org/10.1016/j.yqres.2008.07.002 Published online by Cambridge University Press

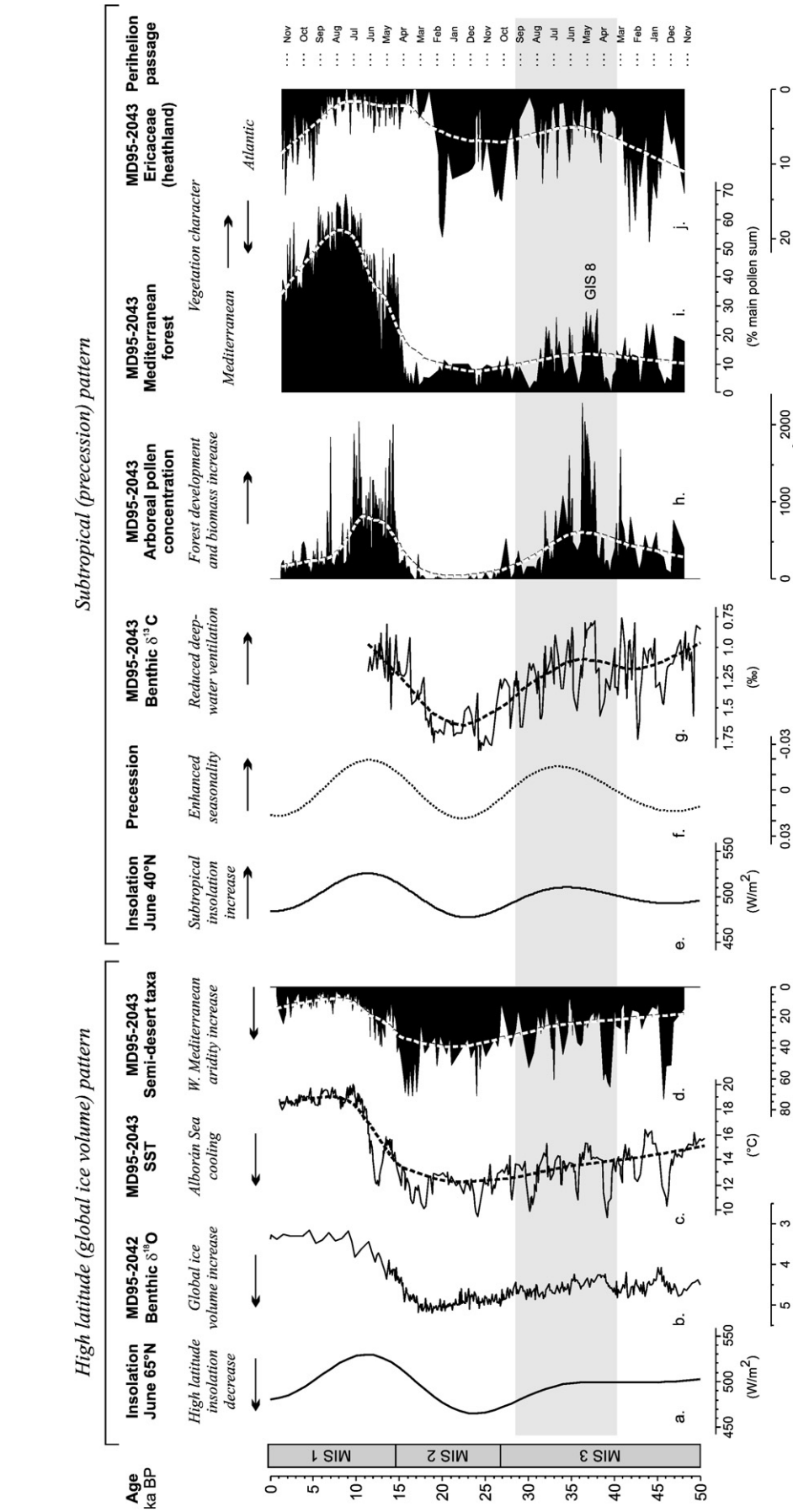

Figure 7. Illustration of long-term patterns in the MD95-2043 record, showing: a. and e.) northern hemisphere summer insolation at 65°N and 40°N (Berger, 1978); b.) benthic oxygen isotope record from MD95-2042, Portuguese margin (Shackleton et al., 2000); c.) Alborán Sea SST reconstruction based on alkenones (Cacho et al., 1999); d., h., i. and j.) pollen percentage and concentration curves (this study); f.) precession index (Laskar et al., 2004); g.) benthic $\delta^{13}C$ (Cacho et al., 2006). Dashed lines through MD95-2043 records are LOWESS curves (α=0.3). Shaded bar highlights the period during which high-latitude and subtropical insolation trends diverge.

https://doi.org/10.1016/j.yqres.2008.07.002 Published online by Cambridge University Press

precipitation in the high altitudinal belts to sustain montane cedar forest development. Although it is recognised that human impact through clearance, pastoral and agricultural activities is likely to have increased during this period, it is considered unlikely that local impacts of prehistoric societies will be detected in the regional vegetation signal contained in the marine pollen record.

Orbital-scale influences on vegetation development

Global ice-volume and insolation impacts

Long-term trends in Alborán SST cooling and semi-desert expansion (indicating climatic aridity) across MIS 3 and 2 parallel the increase of global ice volume as recorded in the benthic $\delta^{18}O$ record from Portuguese margin core MD95-2042 (Shackleton et al., 2000) (Fig. 7). The long-term minimum in Alborán SSTs and maximum semi-desert expansion correspond with maximum ice volume during MIS 2, and lag minimum northern hemisphere summer insolation at high latitudes (the primary control on global ice volume) by ~6 ka (Ruddiman, 2006). These comparisons suggest that the build-up of continental ice sheets during MIS 3 was responsible for a long-term cooling and drying trend in the Alborán region. Increased ice volume may have promoted SST cooling and regional atmospheric aridity through several mechanisms, including reduced intensity of the global hydrological cycle, reduced global temperatures resulting from increased albedo, and intensification of wind systems leading to enhanced sea-surface cooling and evaporative stress on plant life. We note that reduced global atmospheric concentrations of CO_2 during MIS 2 (Petit et al., 1999) may also have promoted the expansion of arid-tolerant vegetation in the Mediterranean due to reduced plant water-use efficiency under low CO_2 conditions (Polley et al., 1993; Cowling and Sykes, 1999; Bennett and Willis, 2000). However, discriminating CO_2 effects from ice-volume impacts in the MD95-2043 pollen record remains very difficult.

Under conditions of minimum ice volume during the Holocene, long-term vegetation changes (semi-desert expansion and Mediterranean forest decline) parallel declining summer insolation (Fig. 7). These trends match the long-term Holocene trend of SST cooling previously identified in the alkenone record by Marchal et al. (2002). In this case, declining summer insolation at subtropical latitudes (40°N) may have been the critical factor for forest decline, impacting on growing season conditions and evaporation/precipitation regimes. The apparent lag between maximum summer insolation and maximum Holocene development of the Mediterranean forest at ~9 cal ka BP may reflect a residual ice-volume effect during the late-glacial period and early Holocene. The general trends observed across the full record are consistent with the view that the amplitude of Mediterranean forest development during glacial periods is related to ice-volume changes while during interglacials forest development is closely related to the amplitude of insolation changes (Tzedakis, 2005).

Precession influence

Long pollen records from the Mediterranean region have revealed the pervasive influence of precession on the Mediterranean vegetation on orbital timescales (Magri and Tzedakis, 2000). A recent examination of marine pollen records from western Europe covering the last climatic cycle has shown that this precession signal is evident in the Mediterranean latitudinal belt and less apparent at higher latitudes (Sánchez Goñi et al., 2008). While the MD95-2043 record only spans two complete precession cycles, and thus does not permit the identification of vegetation response to multiple precession cycles, several features of the record suggest an important modulation of the western Mediterranean climate by precession during this time. An opportunity to discern the influence of precession from other orbital forcing is presented by the precession minimum at around 35 ka BP, which yielded an increase in summer insolation at subtropical latitudes in contrast to trends in high-latitude insolation and ice-volume growth. Several parameters in the MD95-2043 record suggest a long-term precession pattern and, critically, show a similar pattern to subtropical insolation values during MIS 3 (Fig. 7). These include:

(i) Benthic $\delta^{13}C$, which shows trends towards lighter isotopic values near the precession minima. Lighter isotopic values indicate reduced bottom-water ventilation at the site resulting from reduced WMDW formation and a weakening of the Mediterranean thermohaline circulation (Cacho et al., 2006). Reduced WMDW formation in the Gulf of Lions may have resulted from increased precipitation and freshwater runoff into the Mediterranean at this time, as suggested by proxy records of terrigeneous input in a marine sediment core from the Menorca Rise, NW Mediterranean, which show a similar sensitivity to precessional forcing (Frigola et al., 2008). As deep-water formation is principally a winter phenomenon, winter precipitation increases in particular may underline reduced WMSDW formation at this time.

(ii) AP concentrations, which show maxima (minima) associated with precession minima (maxima). The association of low arboreal pollen concentrations and perihelion passage in northern winter is consistent with a documented Mediterranean pattern (Magri and Tzedakis, 2000) observed clearly, for example, in the Valle di Castiglione record (Follieri et al., 1988). While climatic influences on biomass accumulation and pollen production probably underlie this relationship, the pattern may also be reinforced in this record by changes in preservation conditions at the sediment surface. These are also linked to climate via pattern (i), with winter precipitation increases reducing WMDW formation, leading to reduced ventilation of the bottom waters, and increased preservation of organic material (Cacho et al. 2002).

(iii) The amplitude of Mediterranean forest development in MIS 3 during individual D-O warming events (Fig. 7). While semi-desert expansion reflects a long-term ice-volume trend driven by high-latitude insolation decrease, high values for Mediterranean forest during GIS 8, 7, 6 and 5 appear to reflect the maximum in subtropical summer insolation associated with the precession minimum. The same pattern can be detected in the vegetation record of nearby ODP site 976 (Combourieu Nebout et al., 2002) and for SW Iberia from MD95-2042 (Sánchez Goni et al., 2000.), suggesting that this is a robust regional signal for S Iberia. So, while high-latitude insolation and ice-sheet climate impacts appear to govern a long-term aridification trend, expressed most strongly in stadial development of semi-desert vegetation, the development of Mediterranean forest under interstadial conditions was conditioned by low-latitude summer insolation. This precession pattern in forest development is not clearly observed in marine pollen records MD99-2331 and MD95-2039 from the NW Iberian margin (Roucoux et al., 2005; Sánchez Goñi et al., 2008) or the Bay of Biscay (MD04-2845; Sánchez Goñi et al., 2008), suggesting a more important influence of precession on the modulation of vegetation response to abrupt climate events of late MIS 3 in the western Mediterranean basin than in the northern Iberian Peninsula (Sánchez Goñi et al., 2008).

(iv) Contrasts in vegetation composition between different interstadials (Figs. 6 and 7). An important comparison can be drawn between interstadials (GIS) 12 and 8, which fall near a precession maximum and minimum, respectively. Both interstadials were characterised by warm SSTs (15–16°C) sustained over a relatively long duration, and they represent the two strongest phases of mixed oak forest expansion during the period 48–15 ka BP. However, GIS 12 displays an Atlantic, oceanic character with maxima in deciduous *Quercus* and Ericaceae, and GIS 8 a markedly Mediterranean character with

https://doi.org/10.1016/j.yqres.2008.07.002 Published online by Cambridge University Press

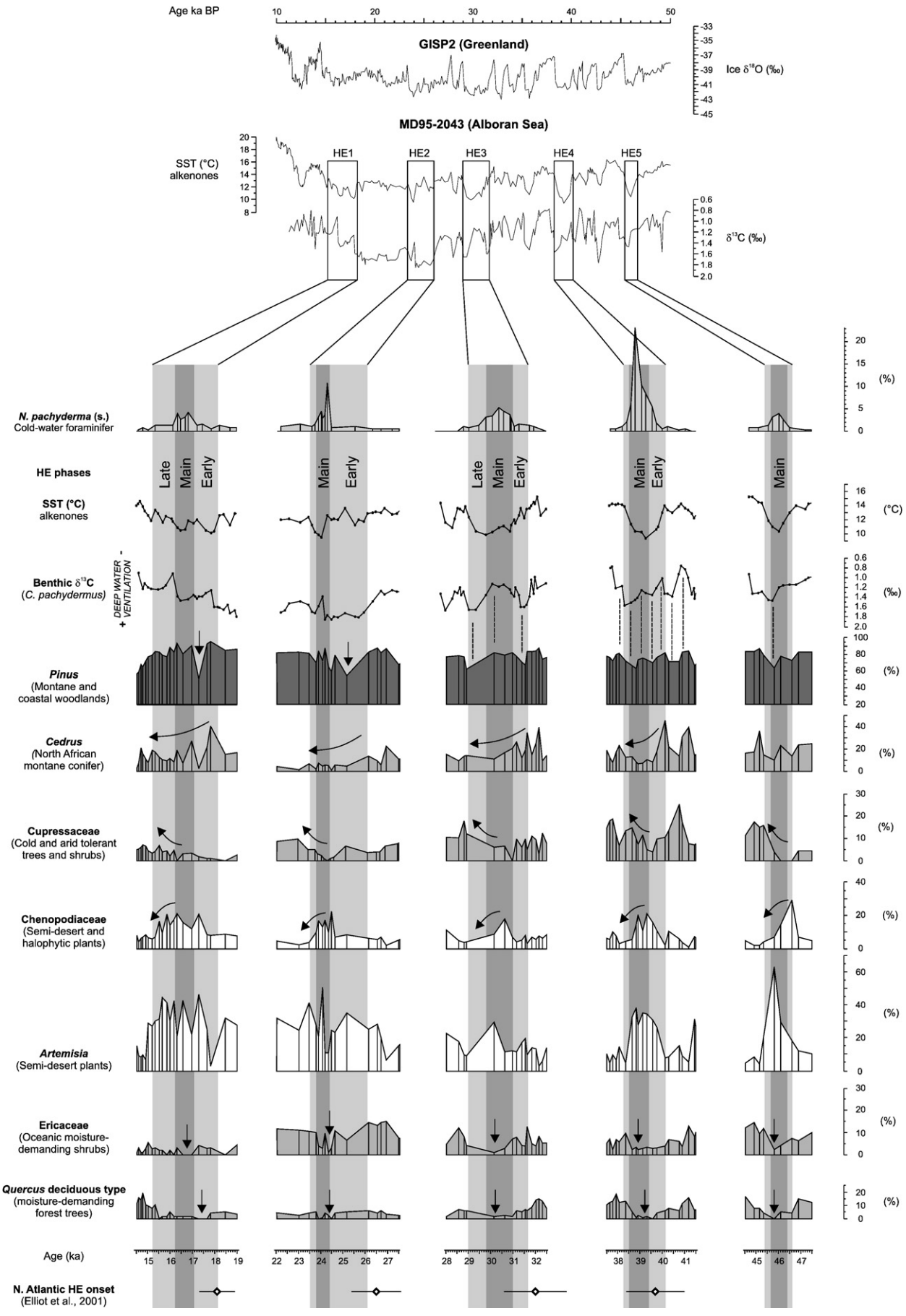

https://doi.org/10.1016/j.yqres.2008.07.002 Published online by Cambridge University Press

stronger development of evergreen *Quercus*, accompanied by occurrences of the most thermophilous oak taxon, *Quercus suber*, as well as *Olea*, *Phillyrea*, *Cistus* and *Coriaria*. The Mediterranean character of GIS 8 probably relates to enhanced seasonal thermal contrasts and associated influences on the seasonal distribution of precipitation (increased winter rains/summer dryness). The same contrast between GIS 12 and GIS 8 is detected at ODP site 976 (Combourieu Nebout et al., 2002), and in the vegetation record of SW Iberia from MD95-2042 (Sánchez Goni et al., 2000). Similar contrasts in vegetation character are also evident in the late-glacial and Holocene record presented here, with higher proportions of evergreen oak near the precession minimum.

(v) Heath development (Fig. 7). Ericaceae, in contrast to the Mediterranean forest taxa, show a consistent relationship with phases of perihelion during the northern hemisphere winter, with higher values occurring during the three precession maxima in the 48 ka record. Values increase with the transition to perihelion passage during autumn (September) and decrease with perihelion passage in spring (March). This relationship suggests a consistent response of the Ericaceae to reduced thermal seasonality and associated changes in the seasonal distribution of rainfall (reduced summer dryness) despite contrasting boundary conditions (during MIS 3, MIS 2 and the late Holocene). This pattern supports evidence for a pervasive precessional control on cycles of heathland development in the Iberian peninsula during MIS 6 (Margari et al., 2007), and during MIS 7, 8 and 9 (Roucoux et al., 2006).

These precession-related patterns probably reflect an enhancement of the essential summer–dry/winter–wet character of the Mediterranean climate during times of perihelion passage in summer (precession minima). Enhanced summer dryness during precession minima in the western Mediterranean may be linked through atmospheric teleconnections to strengthening of the Asian and African summer monsoons. Rodwell and Hoskins (1996, 2001) show that subtropical heating and ascent over south Asia induces adiabatic descent and dry conditions over the eastern Sahara and Mediterranean during summer, part of a global pattern of remote connections through upper level Rossby waves. Raicich et al. (2003) also show teleconnections between the Asian monsoon and the Mediterranean region, suggesting that intensification of monsoon regime is correlated with changes in sea-level pressure gradients in the Mediterranean, which in turn may result in intensification of the Etesian wind regime that brings weak southerly winds to the western Mediterranean. While teleconnections with the Asian monsoon may be most influential in the eastern Mediterranean basin (Ziv et al., 2004), teleconnections with the African monsoon promote summer aridity and warmth in the western Mediterranean basin during times of enhanced west African monsoons (Baldi et al., 2004). Modelling studies also suggest that net precipitation over the Mediterranean basin should increase during precession minima, and that winter precipitation should be favoured by stronger land/sea temperature contrasts over the Mediterranean Sea in autumn as the land cools faster than the sea (Tuenter et al., 2003; Meijer and Tuenter, 2007).

Enhanced summer dryness and winter moisture availability during precession minima can explain the indications in the MD95-2043 record of climatic changes promoting reduced deep-water ventilation and strong development of the Mediterranean forest. The record supports the view that Mediterranean vegetation changes were paced by precession (Magri and Tzedakis, 2000; Sánchez Goñi et al., 2008), although further detailed exploration of longer records from the region is needed to confirm and refine the understanding of precession impacts. Tzedakis (2005, 2007) highlights the role of orbital mean state in the modulation of vegetation response to sub-orbital-scale oscillations. In the MD95-2043 record, an important example of the interaction of orbital- and sub-orbital-scale climate impacts is observed, notably the influence of precession on both the amplitude and vegetation composition of individual interstadials.

Sub-orbital-scale climate impacts on vegetation

North Atlantic climate variability

At sub-orbital timescales, the dominant influence of North Atlantic climate variability is strongly apparent in the MD95-2043 record. Opposing phases of forest development and semi-desert expansion are in phase with SST fluctuations during MIS 3 (Fig. 4), indicating the coupling of atmospheric and oceanic conditions during D-O oscillations and HEs, and the rapid transmission of North Atlantic climate changes into the western Mediterranean region. The response of vegetation in the Alborán borderlands to rapid North Atlantic climate changes is also observed during MIS 2 and 1, with semi-desert expansion during HEs 2 and 1, rapid forest development at the onset of the Bölling-Allerød, and semi-desert expansion during the YD. Strong variability on centennial to millennial scales is also noted in the Holocene pollen record, with systematic fluctuations in Mediterranean forest values indicating short-term atmospheric changes during the Holocene. However, unlike the large amplitude climate events of the glacial and late-glacial periods, atmospheric changes during the Holocene appear to have been less closely coupled to SST fluctuations at the site, as consistent relationships with the record of Alborán SST coolings (AC events; Cacho et al., 2001) are not apparent.

Complex vegetation response to Heinrich Events in the Alborán borderlands

In Figure 8, early, main and late phases are delimited for HEs 5–1 on the basis of *N. pachyderma* (s) percentages, alkenone-derived SSTs and δ^{13}C values. The early phase begins with SST cooling and changes in the δ^{13}C record reflecting increased deep-water formation in the Gulf of Lions. The start of this early phase is chronologically consistent with dates for the start of the HE in the North Atlantic from multiple marine cores (Elliot et al., 2001), as shown in Figure 8. The main phase is defined by peak *N. pachyderma* (s) abundances, corresponding to the main episode of sub-polar water entrance into the Alborán Sea. For HE 3 and HE 2, this entrance of sub-polar waters may also be traced in the δ^{13}C record as a temporary lightening of isotopic values related to a reduction of deep-water formation due to freshening of the surface waters (Cacho et al., 2006). The decline of *N. pachyderma* (s) values marks the start of the late phase, which is characterised by low or rising SSTs and typically by enhanced circulation as during the early phase. This tripartite structure is more or less well-defined for each HE, although some phases are at the limits of sample resolution.

While each HE reveals a slightly different vegetation pattern, some recurring features are observed. During the early phase of HEs 4–1, *Cedrus* values begin high and subsequently decline towards the main and late phases. Peaks in *Cedrus* at the onset of the HEs may represent a transport signal related to an enhancement of southerly winds at the transition to North Atlantic cold events, as previously suggested for the Holocene by Magri and Parra (2002). Bout-

Figure 8. Comparison of marine proxy and pollen taxa records from MD95-2043 for Heinrich events 5–1, showing a tripartite climatic structure for the events. Arrows indicate recurring trends in different taxa within the Heinrich events; dashed lines highlight visual correlations between *Pinus* and benthic δ^{13}C values. Marine proxy data from Cacho et al. (1999, 2006). The date of the onset of the IRD deposition in the northern Atlantic (Elliot et al., 2001) is shown with the associated error for HEs 4–1. GISP2 oxygen isotope curve from Grootes et al. (1993).

https://doi.org/10.1016/j.yqres.2008.07.002 Published online by Cambridge University Press

Roumazeilles et al. (2007) have recently shown the increase of wind-blown inputs of North African origin at ODP site 976 during the HEs, notably with peaks in palygorskite clay minerals accompanied by the presence of *Argania* pollen (a Moroccan endemic taxa), corroborating evidence from MD95-2043 for increased Saharan dust transport to the Alborán Sea during the HEs (Moreno et al., 2002). Peaks in *Cedrus* at the onset of the HEs may be part of the same phenomenon, indicating an intensification of southerly winds bringing North African pollen to the site.

However, while transport signals seem likely, no clear relationship is detected overall between *Cedrus* percentages and sedimentological and geochemical indicators for increased wind strength and Saharan dust transport presented in Moreno et al. (2002). A second hypothesis, supported at least by the good match between periods of high *Cedrus* values with *Cedrus* expansion documented in terrestrial records during the late-glacial and Holocene (Reille, 1977; Salamani, 1993; Lamb and van der Kaars, 1995), is that peaks in *Cedrus* indicate increases in montane forest populations. Extending this second hypothesis, high values of *Cedrus* at the onset of HEs could suggest an expansion or at least survival of cold-tolerant, moisture-demanding montane forest in response to a reduction in winter temperatures and high precipitation, at least in the high altitudinal belts. This hypothesis is consistent with recent evidence from NW Iberia for generally cold but humid conditions during the early part of the HEs, and more strongly arid conditions during a second phase (Naughton et al., 2007b). Whether this scenario may also apply to the Alborán borderlands will require new terrestrial records to confirm the glacial history of montane vegetation in North Africa.

The strongest indications of aridity generally occur during the main phase of the HEs. Chenopodiaceae values reveal similar structured patterns to *N. pachyderma* (s) abundances, with high values in HEs 4–2 associated with the main phase. *Artemisia* also shows maximum values during the main phase; however, peak values typically occur after peak values in Chenopodiaceae (i.e., HEs 5–2) and do not show always the pronounced drop exhibited by Chenopodiaceae values during the late phase (i.e., HEs 2 and 1). Given the halophytic (salt-tolerant) character of many Chenopodiaceae species, this successional pattern within the semi-desert taxa may relate to different patterns of xerophytic vegetation development between the coastal and upland zones, but this altitudinal hypothesis cannot be confirmed without new evidence from terrestrial records. Ericaceae and *Quercus deciduous* type, representing species intolerant of hydric stress, generally reveal minima during the main phase. These taxon specific patterns suggest that maximum aridity was associated with the arrival of sub-polar waters into the Mediterranean, perhaps due to reduced evaporative maritime moisture from the Alborán Sea. However, climatological impacts may also be linked to reduced moisture supply from the eastern North Atlantic following the main arrival of icebergs to the Iberian margin (de Abreu et al. 2003; Voelker et al., 2006; Naughton et al., 2007b).

During the late phase of the HEs, increased values of Cupressaceae suggest increases in vegetation cover perhaps related to the colonisation of xeric habitats (semi-desert plateaux, maritime dunes). Ericaceae and deciduous *Quercus* values increase and Chenopodiaceae values decline from main phase values. These responses suggest slight afforestation under warmer and wetter conditions towards the end of the HE, while wind-driven deep-water formation in the Gulf of Lions generally remained enhanced. A similar late phase with increases in SW Iberian temperate vegetation was described for HEs 5–3 (Sánchez Goni et al., 2000), but has not been detected in NW Iberia where a two-phase pattern of vegetation response is recorded (Naughton et al., 2007a,b). While these comparisons may reflect a N–S difference in HE impacts, further research is needed to understand fully the regional variability of HE impacts in the North Atlantic and Mediterranean regions.

Declines in *Pinus* values are also noted during HEs, being most marked in the early phases of HEs 2 and 1. *Pinus* declines are characteristic of HEs in NW Iberian margin records (Roucoux et al., 2005), where they characterise the early stages of the HE prior to the main arrival of IRD onto the mid-latitude northeastern Atlantic margin and are considered to reflect arboreal declines under cold atmospheric conditions (Naughton et al., 2007a). The interpretation of the declines in the MD95-2043 record is difficult, given not only the characteristic over-representation of *Pinus* in marine records, but also the ecological ambiguity arising from the inclusion of both Mediterranean and montane species in the pollen type. In several instances, correlations between *Pinus* and $\delta^{13}C$ values can be observed, notably during HEs 5, 4 and 3 (Fig. 8). As $\delta^{13}C$ values reflect climatic controls on deep-water formation in the Gulf of Lions including westerly wind strength, the visual correlation between *Pinus* and $\delta^{13}C$ suggests that changing wind conditions may influence the abundances of this well-dispersed and strongly over-represented taxon.

Conclusions

The extended MD95-2043 pollen record reveals vegetation contrasts between MIS 3, 2 and 1. MIS 3 was characterised by the dynamic opposition of mixed *Quercus* forest and semi-desert vegetation in response to D-O and HE climate variability. MIS 2 was characterised by the dominance of semi-desert vegetation, accompanied by shrub vegetation including Ericaceae. The impact of HEs 2 and 1 appears similar to the earlier HEs (5, 4, 3), with climatic conditions more severe than the LGM. MIS 1 was characterised by the maximum development of *Quercus* forest, with rapid afforestation from the onset of the Bölling-Allerød. The YD was marked by semi-desert expansion, but vegetation changes were relatively weaker than those occurring during glacial stadial events. An early to mid-Holocene transition from evergreen to deciduous oak predominance is recorded, and a late Holocene cooling trend. Comparison with the Padul record for the last 25 ka BP confirms the reliability of the extended MD95-2043 record in providing an integrated, regional image of the past vegetation of the Alborán borderlands.

While the record is characterised by high-amplitude changes in response to millennial-scale climate variability, informative orbital-scale trends in vegetation development are observed. The long-term development of semi-desert vegetation during the glacial period followed northern hemisphere insolation and global ice-volume changes, while an interglacial trend of declining arboreal populations reflects decreasing summer insolation. Changes in the seasonality of insolation (precession) also had an important pervasive influence on vegetation development over the last 48,000 yr, influencing both the amplitude and composition of forest development in this Mediterranean region. The findings confirm the key role of precession on the Mediterranean vegetation, including during periods characterised by abrupt, high-amplitude climate changes.

Looking for the first time in detail at taxon specific responses to the last 5 HEs in the western Mediterranean region, a general tripartite climatic pattern emerges that must be confirmed by further high-resolution studies, namely (i) that the onset of the HEs is characterised by increases in *Cedrus* pollen, a signal of cold, humid conditions at altitude and/or enhanced North African wind transport; (ii) that the maximum expansion of semi-desert taxa and decline of moisture-demanding taxa corresponds to the main or middle phase of the HEs, during which time sub-polar waters were entering into the Mediterranean basin; and (iii) that the late phase of the HEs was characterised by a recovery of woody vegetation under less intensely cold and arid conditions.

Acknowledgments

The authors recognise the critical role of IPEV, the IMAGES program and the R/V Marion Dufresne in providing the high-quality core that permitted this research. The authors thank M.-H Castera, O.

Ther and M. Georget for sample and pollen preparation. WJF acknowledges the support of a CNRS post-doctoral research grant. We thank V. Margari and an anonymous reviewer for helpful comments. This study contributes to the EuroCLIMATE project RESOLuTION. This paper is Université Bordeaux 1, UMR-CNRS 5805 EPOC contribution number 1703.

References

Arévalo Barroso, A., 1992. Atlas Nacional de España, Sección II, Grupo 9, Climatología. Madrid, Ministerio de Obras Públicas y Transportes, Dirección General del Instituto Geográfico Nacional.

Baldi, M., Meneguzzo, F., Dalu, G.A., Maracchi, G., Pasqui, M., Capecchi, V., Crisci, A., Piani, F., 2004. Guinea GULF SST and Mediterranean summer climate: analysis of the interannual variability. Bulletin of the American Meteorological Society 4167–4187.

Benabid, A., 2000. Flore et ecosystems du Maroc. Editions Ibis Press, Paris.

Benito Garzón, M., Sánchez de Dios, R., Sainz Ollero, H., 2007. Predictive modelling of tree species distributions on the Iberian Peninsula during the Last Glacial Maximum and Mid-Holocene. Ecography 30, 120–134.

Bennett, K.D., Willis, K.J., 2000. Effect of global atmospheric carbon dioxide on glacial–interglacial vegetation change. Global Ecology and Biogeography 9, 355–361.

Berger, A., 1978. Long-term variations of caloric insolation resulting from the earth's orbital elements. Quaternary Research 9, 139–167.

Bethoux, J.P., 1979. Budgets of the Mediterranean Sea. Their dependence on the local climate and on the characteristics of the Atlantic waters. Oceanologica Acta 2, 157–163.

Bout-Roumazeilles, V., Combourieu Nebout, N., Peyron, O., Cortijo, E., Landais, A., Masson-Delmotte, V., 2007. Connection between South Mediterranean climate and North African atmospheric circulation during the last 50,000 yr BP North Atlantic cold events. Quaternary Science Reviews Volume 26, 3197–3215.

Brewer, S., Cheddadi, R., de Beaulieu, J.-L., Reille, M., Data contributors, 2002. The spread of deciduous *Quercus* throughout Europe since the last glacial period. Forest Ecology and Management 156, 27–48.

Birks, H.J.B., 1998. Numerical tools in palaeolimnology — Progress, potentialities, and problems. Journal of Paleolimnology 20, 307–332.

Cacho, I., Grimalt, J.O., Pelejero, C., Canals, M., Sierro, F.J., Flores, J.A., Shackleton, N.J., 1999. Dansgaard-Oeschger and Heinrich event imprints in Alboran Sea temperatures. Paleoceanography 14, 698–705.

Cacho, I., Grimalt, J.O., Sierro, F.J., Shackleton, N.J., Canals, M., 2000. Evidence for enhanced Mediterranean thermohaline circulation during rapid climatic coolings. Earth and Planetary Science Letters 183, 417–429.

Cacho, I., Grimalt, J.O., Canals, M., Sbaffi, L., Shackleton, N., Schönfeld, J., Zahn, R., 2001. Variability of the western Mediterranean Sea surface temperature during the last 25,000 years and its connection with the northern hemisphere climatic changes. Paleoceanography 16, 40–52.

Cacho, I., Grimalt, J.O., Canals, M., 2002. Response of the Western Mediterranean Sea to rapid climate variability during the last 50,000 years: a molecular biomarker approach. Journal of Marine Systems 33–34, 253–272.

Cacho, I., Shackleton, N., Elderfield, H., Sierro, F.J., Grimalt, J.O., 2006. Glacial rapid variability in deep-water temperature and $d^{18}O$ from the Western Mediterranean Sea. Quaternary Science Reviews 25, 3294–3311.

Carrión, J.S., 2002. Patterns and processes of Late Quaternary environmental change in a montane region of southwestern Europe. Quaternary Science Reviews 21, 2047–2066.

Carrión, J.S., Munuera, M., Dupré, M., Andrade, A., 2001. Abrupt vegetation changes in the Segura Mountains of southern Spain throughout the Holocene. Journal of Ecology 89, 783–797.

Carrión, J.S., Sánchez-Gómez, P., Mota, J.F., Yll, R., Chaín, C., 2003. Holocene vegetation dynamics, fire and grazing in the Sierra de Gádor, southern Spain. The Holocene 13, 839–849.

Carrión, J.S., Yll, E.I., Willis, K.J., Sánchez, P., 2004. Holocene forest history of the eastern plateaux in the Segura mountains (Murcia, southeastern Spain). Review of Palaeobotany and Palynology 132, 219–236.

Carrión, J.S., Fuentes, N., González-Sampériz, P., Sánchez Quirante, L., Finlayson, J.C., Fernández, S., Andrade, A., 2007. Holocene environmental change in a montane region of southern Europe with a long history of human settlement. Quaternary Science Reviews 26, 1455–1475.

Cleveland, W.S., 1979. Robust locally weighted regression and smoothing scatterplots. Journal of the American Statistical Association 74, 829–836.

Colmenero-Hidalgo, E., Flores, J.-A., Sierro, F.J., Bárcena, M.A., Löwemark, L., Schönfeld, J., Grimalt, J.O., 2004. Ocean surface water response to short-term climate changes revealed by coccolithophores from the Gulf of Cadiz (NE Atlantic) and Alboran Sea (W Mediterranean). Palaeogeography, Palaeoclimatology, Palaeoecology 205, 317–336.

Combourieu Nebout, N., Turon, J.-L., Zahn, R., Capotondi, L., Londeix, L., Pahnke, K., 2002. Enhanced aridity and atmospheric high-pressure stability over the western Mediterranean during the North Atlantic cold events of the past 50 k.y. Geology 30, 863–866.

Cowling, S.A., Sykes, M.T., 1999. Physiological significance of low atmospheric CO_2 for plant-climate interactions. Quaternary Research 52, 237–242.

de Abreu, L., Shackleton, N.J., Schönfeld, J., Hall, M., Chapman, M.R., 2003. Millennial-scale oceanic climate variability off the Western Iberian margin during the last two glacial periods. Marine Geology 196, 1–20.

Elliot, M., Labeyrie, L., Dokken, T., Manthé, S., 2001. Coherent patterns of ice-rafted debris deposits in the Nordic regions during the last glacial (10–60 ka). Earth and Planetary Science Letters 194, 151–163.

Fabrés, J., Calafat, A., Sanchez-Vidal, A., Canals, M., Heussner, S., 2001. Composition and spatial variability of particle fluxes in the Western Alboran Gyre, Mediterranean Sea. Journal of Marine Systems 33–34, 431–456.

Fernández, S., Fuentes, N., Carrión, J.S., González-Sampériz, P., Montoya, E., Gil, G., Vega-Toscano, Riquelme, J., 2007. The Holocene and Upper Pleistocene pollen sequence of Carihuela Cave, southern Spain. Geobios 40, 75–90.

Fletcher, W., Boski, T., Moura, D., 2007. Palynological evidence for environmental and climatic change in the lower Guadiana valley (Portugal) during the last 13,000 years. The Holocene 17, 479–492.

Follieri, M., Magri, D., Sadori, L., 1988. 250,000 year pollen record from Valle di Castiglione (Roma). Pollen et Spores 30, 329–356.

Frigola, J., Moreno, A., Cacho, I., Canals, M., Sierro, F.J., Flores, J.A., Grimalt, J.O., 2008. Evidence of abrupt changes in Western Mediterranean Deep Water circulation during the last 50 kyr: a high-resolution marine record from the Balearic Sea. Quaternary International 181, 88–104.

Grootes, P.M., Stuiver, M., White, J.W.C., Johnsen, S., Jouzel, J., 1993. Comparison of oxygen isotope records from the GISP2 and GRIP Greenland ice cores. Nature 366, 552–554.

Heusser, L.E., Balsam, W.L., 1977. Pollen distribution in the northeast Pacific Ocean. Quaternary Research 7, 45–62.

Hooghiemstra, H., Lézine, A.-M., Leroy, S.A.G., Dupont, L., Marret, F., 2006. Late Quaternary palynology in marine sediments: a synthesis of the understanding of pollen distribution patterns in the NW African setting. Quaternary International 148, 29–44.

Hughen, K.A., Baillie, M.G.L., Bard, E., Bayliss, A., Beck, J.W., Bertrand, C., Blackwell, P.G., Buck, C.E., Burr, G., Cutler, K.B., Damon, P.E., Edwards, R.L., Fairbanks, R.G., Friedrich, M., Guilderson, T.P., Kromer, B., McCormac, F.G., Manning, S., Bronk Ramsey, C., Reimer, P.J., Reimer, R.W., Remmele, S., Southon, J.R., Stuiver, M., Talamo, S., Taylor, F.W., van der Plicht, J., Weyhenmeyer, C.E., 2004. Marine04 marine radiocarbon age calibration, 0–26 Cal Kyr BP. Radiocarbon 46, 1059–1086.

Kageyama, M., Combourieu Nebout, N., Sepulchre, P., Peyron, O., Krinner, G., Ramstein, G., Cazet, J.-P., 2005. The Last Glacial Maximum and Heinrich Event 1 in terms of climate and vegetation around the Alboran Sea: a preliminary model-data comparison. Comptes Rendus Geosciences 337, 983–992.

Kucera, M., Rosell-Melé, A., Schneider, R., Waelbroeck, C., Weinelt, M., 2005. Multiproxy approach for the reconstruction of the glacial ocean surface (MARGO). Quaternary Science Reviews 24, 813–819.

Lamb, H., van der Kaars, S., 1995. Vegetational response to Holocene climatic change: pollen and palaeolimnological data from the Middle Atlas, Morocco. The Holocene 5, 400–408.

Laskar, J., Robutel, P., Joutel, F., Gastineau, M., Correia, A.C.M., Levrard, B., 2004. A long-term astronomical solution for the insolation quantities of the Earth. Astronomy and Astrophysics 428, 261–285.

López de Heredia, U., Carrión, J.S., Jiménez, P., Collada, C., Gil, L., 2007. Molecular and palaeoecological evidence for multiple glacial refugia for evergreen oaks on the Iberian Peninsula. Journal of Biogeography 34, 1505–1517.

Magri, D., Parra, I., 2002. Late Quaternary western Mediterranean pollen records and African winds. Earth and Planetary Science Letters 200, 401–408.

Magri, D., Tzedakis, P.C., 2000. Orbital signatures and long-term vegetation patterns in the Mediterranean. Quaternary International 73/74, 69–78.

Maher, L.J., 1972. Nomograms for computing 95% limits of pollen data. Review of Palynology and Palaeobotany 13, 85–93.

Marchal, O., Cacho, I., Stocker, T.F., Grimalt, J.O., Calvo, E., Martrat, B., Shackleton, N., Vautravers, M., Cortijo, E., van Kreveld, S., Andersson, C., Ko, N., Chapman, M., Sbaffi, L., Duplessy, J.-C., Sarnthein, M., Turon, J.-L., Duprat, J., Jansen, E., 2002. Apparent long-term cooling of the sea surface in the northeast Atlantic and Mediterranean during the Holocene. Quaternary Science Reviews 21, 455–483.

Margari, V., Tzedakis, P.C., Shackleton, N.J., Vautravers, M., 2007. Vegetation response in SW Iberia to abrupt climate change during MIS 6: direct land-sea comparisons. Quaternary International 167–168 (Supplement 1), 267–268.

Meijer, P.Th., Tuenter, E., 2007. The effect of precession-induced changes in the Mediterranean freshwater budget on circulation at shallow and intermediate depth. Journal of Marine Systems 68, 349–365.

Millot, C., 1999. Circulation in the Western Mediterranean Sea. Journal of Marine Systems 20, 423–442.

Mix, A.C., Bard, E., Schneider, R., 2001. Environmental processes of the ice age: land, oceans, glaciers (EPILOG). Quaternary Science Reviews 20, 627–657.

Moreno, A., Cacho, I., Canals, M., Prins, M.A., Sánchez -Goni, M.-F., Grimalt, J.O., Weltje, G.J., 2002. Saharan dust transport and high-latitude glacial climatic variability: the Alboran Sea record. Quaternary Research 58, 318–328.

Mudie, P.J., Rochon, A., Aksu, A.E., 2002. Pollen stratigraphy of Late Quaternary cores from Marmara Sea: land-sea correlation and paleoclimatic history. Marine Geology 190, 233–260.

Mudie, P.J., McCarthy, F.M., 2006. Marine palynology: potentials for onshore-offshore correlation of Pleistocene-Holocene records. Transactions of the Royal Society of South Africa 61, 139–157.

Naughton, F., Sánchez Goni, M.F., Desprat, S., Turon, J.L., Duprat, J., Malaizé, B., Joli, C., Cortijo, E., Drago, T., Freitas, M.C., 2007a. Present-day and past (last 25 000 years) marine pollen signal off western Iberia. Marine Micropaleontology 62, 91–114.

Naughton, F., Sánchez Goñi, M.F., Turon, J.-L., Duprat, J., Cortijo, E., Malaizé, B., Joli, C., Bard, E. and Rostek, F., 2007b. Wet to dry climatic trend in north western Iberia within Heinrich events. IX International Conference on Paleoceanography (ICP9), September 2007, Shanghai (China).

Olalde, M., Herrán, A., Espinel, S., Goicoechea, P.G., 2002. White oaks phylogeography in the Iberian Peninsula. Forest Ecology and Management 156, 89–102.
Pantaléon Cano, J., Yll, E.I., Pérez-Obiol, R., Roure, J.M., 2003. Palynological evidence for vegetational history in semi-arid areas of the western Mediterranean (Almería, Spain). The Holocene 13, 109–119.
Peinado Lorca, M., Rivas-Martinez, S., 1987. *La vegetación de España*. Universidad de Alcala de Henares, Secretaria general, Servicio de publicaciones.
Pérez-Folgado, M., Sierro, F.J., Flores, J.A., Cacho, I., Grimalt, J.O., Zahn, R., Shackleton, N., 2003. Western Mediterranean planktonic foraminifera events and millennial climatic variability during the last 70 kyr. Marine Micropalaeontology 48, 49–70.
Petit, J.R., Jouzel, J., Raynaud, D., Barkov, N.I., Barnola, J.-M., Basile, I., Bender, M., Chappellaz, J., Davis, M., Delaygue, G., Delmotte, M., Kotlyakov, V.M., Legrand, M., Lipenkov, V.Y., Lorius, C., Pépin, L., Ritz, C., Saltzman, E., Stievenard, M., 1999. Climate and atmospheric history of the past 420,000 years from the Vostok ice core, Antarctica. Nature 399, 429–436.
Polley, H.W., Johnson, H.B., Marino, B.D., Mayeux, H.S., 1993. Increase in C3 plant water-use efficiency and biomass over Glacial to present CO_2 concentrations. Nature 361, 61–64.
Pons, A., Reille, M., 1988. The Holocene and Upper Pleistocene pollen record from Padul (Granada, Spain): a new study. Palaeogeography, Palaeoclimatology, Palaeoecology 66, 243–263.
Quezel, P., 2002. Réflexions sur l'évolution de la flore et de la végétation au Maghreb méditerranéen. Ibis Press, Paris.
Reille, M., 1977. Contribution pollenanalytique à l'histoire holocène de la végétation des montagnes du Rif (Maroc septentrional). Recherches Françaises sur le Quaternaire 1, 53–76.
Raicich, F., Pinardi, N., Navarra, A., 2003. Teleconnections between Indian monsoon and Sahel rainfall and the Mediterranean. International Journal of Climatology 23, 173–186.
Rodwell, M.J., Hoskins, B.J., 1996. Monsoons and the dynamics of deserts. Quarterly Journal of the Royal Meteorological Society 122, 1385–1404.
Rodwell, M.J., Hoskins, B.J., 2001. Subtropical anticyclones and summer monsoons. Journal of Climate 14, 3192–3211.
Roucoux, K.H., de Abreu, L., Shackleton, N.J., Tzedakis, P.C., 2005. The response of NW Iberian vegetation to North Atlantic climate oscillations during the last 65 kyr. Quaternary Science Reviews 24, 1637–1653.
Roucoux, K.H., Tzedakis, P.C., de Abreu, L., Shackleton, N.J., 2006. Climate and vegetation changes 180,000 to 345,000 years ago recorded in a deep-sea core off Portugal. Earth and Planetary Science Letters 249, 307–325.
Ruddiman, W.F., 2006. Orbital changes and climate. Quaternary Science Reviews 25, 3092–3112.
Salamani, M., 1993. Premières données paléophytogéographiques du Cèdre de l'Atlas (*Cedrus atlantica*) dans la région de Grande Kabylie (NE Algérie). Palynosciences 2, 147–155.
Sánchez Goni, M.F., Turon, J.L., Eynaud, F., Gendreau, S., 2000. European climatic response to millenial-scale changes in the atmosphere-ocean system during the Last Glacial period. Quaternary Research 54, 394–403.
Sánchez Goñi, M.F., Cacho, I., Turon, J.-L., Guiot, J., Sierro, F.J., Peypouquet, J.-P., Grimalt, J.O., Shackleton, N.J., 2002. Synchroneity between marine and terrestrial responses to millennial scale climatic variability during the last glacial period in the Mediterranean region. Climate Dynamics 19, 95–105.
Sánchez Goñi, M.F., Landais, A., Fletcher, W.J., Naughton, F., Desprat, S., Duprat, J., 2008. Evidence for major sources of CH_4 in northern mid-low latitudes during the last glacial. Quaternary Science Reviews 27, 1136–1151.
Shackleton, N.J., Hall, M.A., Vincent, E., 2000. Phase relationships between millennial scale events 64,000–24,000 years ago. Paleoceanography 15, 565–569.
Sierro, F.J., Hodell, D.A., Curtis, J.H., Flores, J.A., Reguera, I., Colmenero-Hidalgo, E., Bárcena, M.A., Grimalt, J.O., Cacho, I., Frigola, J., Canals, M., 2005. Impact of iceberg melting on Mediterranean thermohaline circulation during Heinrich events. Paleoceanography 20, PA2019 doi:10.1029/2004PA001051.
Stuiver, M., Reimer, P.J., 1993. Extended ^{14}C database and revised CALIB radiocarbon calibration program. Radiocarbon 35, 215–230.
Tuenter, E., Weber, S.L., Hilgen, F.J., Lourens, L.J., 2003. The response of the African summer monsoon to remote and local forcing due to precession and obliquity. Global and Planetary Change 36, 219–235.
Turon, J.-L., 1984. Le paynoplancton dans l'environnement actuel de l' Atlantique nord-oriental. Evolution climatique et hydrologique depuis le dernier maximum glaciaire. PhD thesis, Bordeaux 1 University, France.
Tzedakis, P.C., 2005. Towards an understanding of the response of southern European vegetation to orbital and suborbital climate variability. Quaternary Science Reviews 24, 1585–1599.
Tzedakis, P.C., 2007. Seven ambiguities in the Mediterranean palaeoenvironmental narrative. Quaternary Science Reviews 26, 2042–2066.
Voelker, A.H.L., Lebreiro, S.M., Schonfeld, J., Cacho, I., Erlenkeuser, H., Abrantes, F., 2006. Mediterranean outflow strengthening during northern hemisphere coolings: a salt source for the glacial Atlantic? Earth and Planetary Science Letters 245, 39–55.
Ziv, B., Saaroni, H., Alpert, P., 2004. Factors governing the summer regime of the eastern Mediterraneaen. International Journal of Climatology 24, 1859–1871.